

FLOW OVER OGEE SPILLWAY: PHYSICAL AND NUMERICAL MODEL CASE STUDY

By Bruce M. Savage¹ and Michael C. Johnson,² Members, ASCE

ABSTRACT: A study was completed to compare flow parameters over a standard ogee-crested spillway using a physical model, numerical model, and existing literature. The physical model was constructed of Plexiglas and placed in a test flume. Pressure taps were installed along the entire length of the spillway. Discharge and pressure data were recorded for 10 different flow conditions. A commercially available computational fluid dynamics (CFD) program, which solves the Reynolds-averaged Navier-Stokes equations, was used to model the physical model setup. Data interpolated from U.S. Bureau of Reclamation and U.S. Army Corps of Engineers design nomographs provided discharge and pressure data from the literature. Nondimensional discharge curves are used to compare the results from the different methods. Pressures are compared at low, mid, and high flow conditions. It is shown that there is reasonably good agreement between the physical and numerical models for both pressures and discharges. The availability and power of existing numerical methods provides engineers with another tool in the design and analysis of ogee spillways.

INTRODUCTION

The ogee-crested spillway, because of its superb hydraulic characteristics, has been one of the most studied hydraulic structures. Its ability to pass flows efficiently and safely, when properly designed, with relatively good flow measuring capabilities, has enabled engineers to use it in a wide variety of situations. Although much is understood about the general ogee shape and its flow characteristics, it is also understood that a deviation from the standard design parameters such as a change in upstream flow conditions, slightly modified crest shape, or construction variances can change the flow properties. These small changes often require engineers to evaluate the crest and determine whether or not the change or deviation will be detrimental to the spillway's performance. Such is the case when an updated probable maximum flood calculation requires a spillway to pass a larger flow than it was designed to handle.

With the rapidly changing advances in computational modeling for solving the governing equations of fluid flow, engineers now face the decision of which method(s) to use in evaluating existing and proposed spillway designs. The choice of a physical model, computational model, or interpolating/extrapolating the needed information from the U.S. Army Corps of Engineers (USACE) or the U.S. Bureau of Reclamation (USBR) design/performance curves can be a daunting task. This is especially true if an engineer is unfamiliar with the capabilities and limitations of state-of-the-art computational modeling or if the effects of extrapolating are not fully understood and thereby one method cannot be justified over the other.

To assist the engineer in the decision about which methodology to pursue, this study was completed at the Utah Water Research Laboratory (UWRL) to compare the discharge and crest pressures from flow over an uncontrolled ogee-crested spillway using a physical model, computational model, and design curves from the USBR and USACE.

To correlate this study with existing USBR and USACE

data, a standard ogee-crested spillway design (Maynard 1985) was used. The crest geometry is shown in Fig. 1. The physical model was constructed of molded Plexiglas to accurately represent the desired shape. A computer generated object of the crest shape was imported into the commercially available computational fluid dynamics (CFD) software package, Flow-3D. Using nondimensional design parameters, performance data were interpolated from USACE (1990) and USBR (*Design* 1977) published reports.

BACKGROUND

In theory, the ogee-crested spillway's performance attributes are due to its shape being derived from the lower surface of an aerated nappe flowing over a sharp-crested weir. The ogee shape results in near-atmospheric pressure over the crest section for a single given upstream head. Because the flow rate is not limited to a single head, the flow rate over an ogee-crested spillway varies from that of a sharp-crested weir. At heads lower than the design head, the discharge is less because of crest resistance. At higher heads, the discharge is greater than an aerated sharp-crested weir because the negative crest pressure suction more flow. Designing a crest that allows small negative pressures at the design flow is a practice called underdesigning and it increases the efficiency of the spillway. However, the crest pressures must not be allowed to go too negative. A large negative pressure on the crest can cause cavitation damage, destabilization of the structure, and possible failure. Large negative pressures can also be caused by discontinuities in the crest shape.

Considerable research has been done to determine the shape of the crest of an overflow spillway, and different methods are available that depend on the relative height and upstream face slope of the spillway (Maynard 1985). Bazin (Chow 1959), in 1888, completed a comprehensive laboratory investigation and was the first to study the ogee shape. After Bazin, the majority of the existing information is derived from extensive data taken from physical models completed by the USBR and the USACE. Because this paper is not intended to be a compendium of the literature and the design criteria, the reader is referred to the following references for more information: USACE (1990), Maynard (1985), *Design* (1977), Murphy (1973), and Chow (1959).

In the past few years, several researchers have attempted to solve this and similar problems with a variety of mathematical models and computational methods. The main difficulty of the problem is that the flow transitions from subcritical to supercritical flow. In addition, the discharge is unknown and must be solved as part of the solution. This is especially critical

¹Grad. Res. Asst., Utah Water Res. Lab., Dept. of Civ. Engrg., Utah State Univ., Logan, UT 84322-8200.

²Adjunct Prof., Utah Water Res. Lab., Dept. of Civ. Engrg., Utah State Univ., Logan, UT 84322-8200.

Note. Discussion open until January 1, 2002. To extend the closing date one month, a written request must be filed with the ASCE Manager of Journals. The manuscript for this paper was submitted for review and possible publication on June 13, 2000; revised April 23, 2001. This paper is part of the *Journal of Hydraulic Engineering*, Vol. 127, No. 8, August, 2001. ©ASCE, ISSN 0733-9429/01/0008-0640-0649/\$8.00 + \$.50 per page. Paper No. 22378.

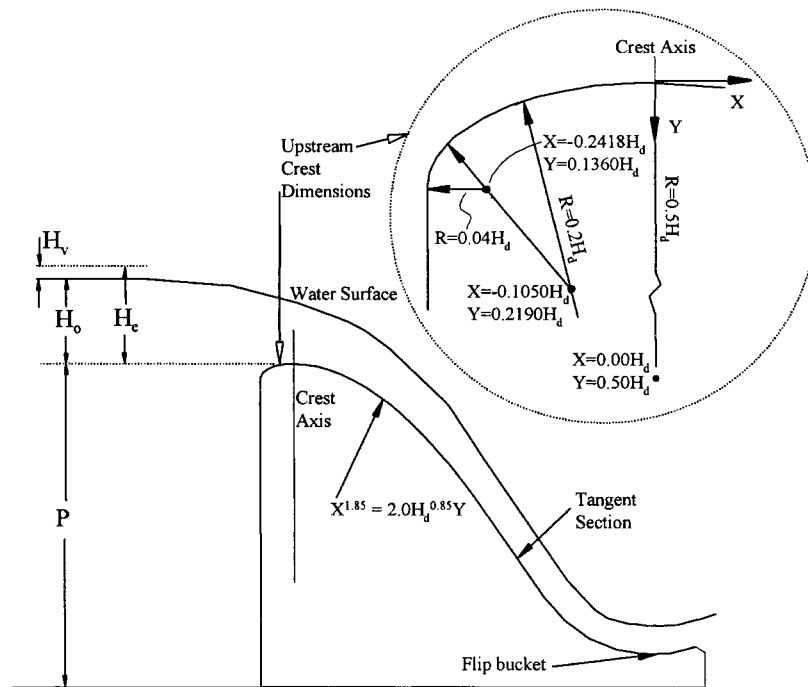


FIG. 1. Ogee Dimensions and Flow Parameters

when the velocity head upstream from the spillway is a significant part of the total upstream head.

An early attempt at modeling spillway flows was completed by Cassidy (1965). By using potential flow theory and mapping into the complex potential plane, he was able to solve for the free surface and crest pressures and found good agreement with experimental data for a limited number of solutions. The close agreement led Cassidy to conclude that viscosity has a negligible influence on the location of the free surface. He also concluded that the point of minimum pressure for a given head is dependent on the boundary configuration. Better convergence of Cassidy's solution was obtained by Ikegawa and Washizu (1973) and Betts (1979) using linear finite elements and the variation principle. Li et al. (1989) completed additional improvements on the 2D irrotational gravity flow by using higher-order elements to model the curved water surface and spillway surface.

More recently, Guo et al. (1998) expanded on the potential flow theory by applying the analytical functional boundary-value theory with the substitution of variables to derive non-singular boundary integral equations. This method was applied successfully to spillways with a free drop. Bürgisser and Rutschmann (1999) used finite elements and an eddy viscosity to iteratively solve the incompressible 2D vertical steady Reynolds-averaged Navier-Stokes (RANS) equations. Given a flow rate, they successfully computed the free surface and velocity and pressure fields using a finite-element grid that adapts locally for a changing water surface. Olsen and Kjellesvig (1998) also included viscous effects by numerically solving the RANS equations in two and three dimensions, using the standard k - ϵ equations (Rodi 1980) to model turbulence. Olsen and Kjellesvig (1998) showed excellent agreement for water surfaces and discharge coefficients for a limited number of flows. However, pressure data were only recorded at five locations downstream from a nonstandard crest at one flow and showed some variability.

The present study approaches the problem numerically using the RANS equations. Ten different flow rates are used to calculate a discharge rating curve for a single crest design, $P/H_d = 2.70$, where P is the dam height and H_d is the design head over the dam. Crest pressures are compared at three dif-

ferent flow rates. Furthermore, the pressures are compared over the entire length of the spillway, including the flip bucket. Although there seems to be considerable data in the literature of crest pressures up to the tangent section located at $X/H_d = 1.4$ and at flip buckets, there is a dearth of information on pressures extending from the tangent section to the flip bucket. These pressures are required if one intends to complete an overall stability analysis of the dam.

GENERAL CREST INFORMATION

In the history of the ogee-crest dam, it is interesting to note the different designs and shapes that have been used. It appears that the majority of these changes have been focused on the crest section upstream from the crest axis. This is logical in that the forward crest is where the flow makes a transition from subcritical to supercritical. Maynard's report (1985) shows four different shapes for vertical face dams. Counter to the upstream section, the downstream section from the crest axis to the tangent section has been "standardized" to the equation shown in Fig. 1. However, the coefficients and exponents may change, depending on the dam geometry and design flow rate.

The general nondimensional equation for discharge is given by

$$Q = \frac{2}{3} C_0 \sqrt{2g} L H_c^{3/2} \quad (1)$$

where Q = total discharge; L = lateral crest length or width; H_c = total head upstream from the crest; g = gravitational constant; and C_0 = discharge coefficient. Note that H_c , the total head, includes the velocity head. Usually, this requires that an iterative solution be completed because the velocity head is not known until the flow rate is calculated. However, because the velocity head is generally a small part of the total head, the equation converges to a solution after several iterations.

The discharge coefficient C_0 is not constant. It is influenced by a variety of factors including the depth of approach, relation of the actual crest shape to the ideal nappe shape, upstream face slope, downstream apron interference, and downstream submergence (Design 1977). Each of the conditions have

ranges and design curves that describe the effect of the parameters mentioned.

NUMERICAL METHODOLOGY

The commercially available CFD package Flow-3D uses the finite-volume method to solve the RANS equations. The computational domain is subdivided using Cartesian coordinates into a grid of variable-sized hexahedral cells. For each cell, average values for the flow parameters (pressure and velocity) are computed at discrete times using a staggered grid technique (Versteeg and Malalasekera 1995). The staggered grid places all dependent variables at the center of each cell with the exception of the velocities u , v , and w and the fractional areas A_x , A_y , and A_z . Velocities and fractional areas are located at the center of cell faces (not cell centers) normal to their associated direction. For example, u and A_x are located at the center of the cell faces that are located in the Y,Z -plane (normal to the X -axis). A two-equation renormalized group theory model, as outlined by Yakhot and Orszag (1986) and Yakhot and Smith (1992), was used for turbulence closure.

The modeling of a free-surface flow over an obstacle with Flow-3D constrains the makeup of each cell within the grid to one of five conditions: completely solid, part solid and fluid, completely fluid, part fluid, and completely empty. The ogee-crested spillway was defined as an obstacle in the rectangular domain by the implementation of the Fractional Area/Volume Obstacle Representation (FAVOR) method. The free surface was computed using a modified volume-of-fluid (VOF) method.

Obstacle Generation

The FAVOR method, outlined by Hirt and Sicilian (1985) and Hirt (1992), is a porosity technique used to define obstacles. The grid porosity value is zero within obstacles and 1 for cells without the obstacle. Cells only partially filled with an obstacle have a value between zero and 1, based on the percent volume that is solid. Therefore, the ogee crest's surface is defined by cells within the grid that have a porosity value between 1 and zero. The location of the interface in each cell is defined as a first-order approximation—a straight line in two dimensions and a plane in three dimensions, determined by the points where the obstacle intersects the cell faces. The slicing plane not only defines the fractional volume that can contain fluid but also determines the fraction area (A_x , A_y , and A_z) on each cell face through which flux (fluid flow) can occur. This method eliminates the “stair-stepping” effect normally associated with rectangular grids and replaces all obstacle surfaces, curved or otherwise, with short, straight-lined segments. In essence, the ogee crest is constructed of a series of short chords that define the ogee's curves. Given this fact, it is obvious that smaller size cells produce a much smoother numerical obstacle boundary. It is important to note that, although short chords can effectively approximate a curved surface, it is still an approximation to a curved surface. To fit a curved surface exactly, a different numerical method such as a second-order finite-element method or a curvilinear boundary fitted method would be required.

Free Surface

To numerically solve the rapidly varying flow over an ogee crest, it is important that the free surface be accurately tracked. Tracking involves three parts: locating the surface, defining the surface as a sharp interface between the fluid and air, and applying boundary conditions at the interface.

One means of tracking the free surface is the VOF method. The VOF method evolved from the marker-and-cell method

(Harlow and Welsh 1965) but is more computationally efficient. The VOF method is described in Nichols and Hirt (1975), Nichols et al. (1980), and Hirt and Nichols (1981). Recent published work on the VOF method includes Kothe and Mjolsness (1992), Yamada and Takikawa (1999), and Colletta et al. (1999).

The VOF method is similar to the FAVOR method in defining cells that are empty, full, or partially filled with fluid. Cells without fluid have a value of zero. Full cells are assigned a value of 1 and partially filled cells have a value between zero and 1. The slope of the free surface within the partial cells is found by an algorithm that uses the surrounding cells to define a surface angle and a surface location. The VOF method allows for steep fluid slopes and breaking waves. Similar to the FAVOR method, the free surface is defined by a series of connected chords (2D) or by connected planes (3D); however, the VOF method allows for a changing free surface over time and space. Once again, this first-order approximation is not an exact fit to the curved flow surface. A true fit would require a second-order or higher adaptive grid that changes temporally and spatially to fit the changing water surface.

The VOF method has additional concerns that require special consideration. VOF numerical techniques tend to be dissipative in nature, which can smear the free surface interface. Smearing of the interface distributes small amounts of fluid across several adjacent cells. These “misty” cells can introduce spurious results and prevent the free surface from being accurately identified. Flow-3D reduces this problem by implementing an algorithm to effectively clean up the misty regions (Flow-3D 1999). The implementation of this algorithm eliminates fluid in the misty regions and resets the fluid fraction in interface cells, thereby not completely adhering to the conservation of mass principle. The conservation of mass principle is additionally violated by computer roundoff error, as the code tracks fluid flux through cell face areas. However, the code also tracks the volume of fluid that is eliminated or added to the solution by the different algorithms. This cumulative volume error can provide a means of monitoring and evaluating the solution accuracy. In the final run of each numerical simulation, a cumulative volume error of less than $\pm 0.03\%$ was reported. Therefore it is believed that the effect on continuity was not significant, for all practical purposes.

Governing Equations and Computational Scheme

The general governing RANS and continuity equations for noncompressible flow, including the VOF and FAVOR variables, are outlined in (2) and (3):

Continuity:

$$\frac{\partial}{\partial x}(uA_x) + \frac{\partial}{\partial y}(vA_y) + \frac{\partial}{\partial z}(wA_z) = 0 \quad (2)$$

Momentum:

$$\frac{\partial U_i}{\partial t} + \frac{1}{V_F} \left(U_j A_j \frac{\partial U_i}{\partial x_j} \right) = \frac{1}{\rho} \frac{\partial P'}{\partial x_i} + g_i + f_i \quad (3)$$

The variables u , v , and w represent the velocities in the x -, y -, and z -directions; V_F = volume fraction of fluid in each cell; A_x , A_y , and A_z = fractional areas open to flow in the subscript directions; ρ = density; P' is defined as the pressure; g_i = gravitational force in the subscript direction; and f_i represents the Reynolds stresses for which a turbulence model is required for closure. It can be seen that, in cells completely full of fluid, V_F and A_j (cell face areas) equal 1, thereby reducing the equations to the basic incompressible RANS equations.

Numerical Model Implementation

A rectangular grid was defined as approximately 3.9 m long by 1.2 m high. The obstacle representing the ogee-crest dam was placed 1.52 m downstream. This placed the upstream boundary away from drawdown effects. Although the physical model was 2D in nature (sectional), one flow rate was numerically modeled in three dimensions to allow comparison of the 2D solution with the full 3D solution. This comparison indicated that the flow was effectively 2D; therefore, all sequential calculations were completed quasi-two-dimensionally (unit thickness in y -direction) to save on computational time.

To speed up convergence to a steady-state solution, a manual multigrid method was implemented. The use of an initial coarse grid ($\Delta x = \Delta y = \Delta z = 24$ mm) allowed an approximate water surface and flow rate to be quickly calculated. A sequential finer grid was then initialized by interpolating the previous calculated values onto the grid. Starting the new grid with the old values allowed the new solution to converge quicker. This manual multigrid method allowed the progression of grid convergence to be noted for each flow.

Grid convergence was found at a uniform cell size of approximately $\Delta x = \Delta y = \Delta z = 12.2$ mm for the mid to higher flows. Fig. 2 shows the grid surrounding the ogee-crested spillway. At lower flows, due to the shallow flow depth over the crest, a smaller cell size, approximately 7.6 mm, was required for grid convergence. To simplify grid construction and the number of numerical variables, a uniform cell size was used throughout this study. Note that use of a variable 3D mesh may be a viable option to decrease the computation time. A variable mesh allows improved resolution in regions where flow variables are rapidly changing and larger cells where resolution is not required. However, caution should be applied when using variable mesh—a rapid change in cell sizes can result in reduced numerical accuracy. For example, a large change between adjacent cell sizes will reduce a numerical second-order accuracy to a first-order accuracy. This problem is outlined in Hirt and Nichols (1981).

Boundary Conditions

To simulate a given flow, it is important that the boundary conditions accurately represent what is physically occurring. Because the flow domain is defined as a hexahedral in Cartesian coordinates, there are six different boundaries on the mesh to be fixed, plus the obstacle surface. To handle mesh boundary conditions, the program adds fictitious boundary cells to the grid with their values either fixed at a given value or updated as the calculations continue. The boundaries on the mesh and their coordinate directions were set as follows: sidewalls y —free slip/symmetry; top z —pressure boundary with gauge pressure equal to zero (atmospheric); bottom z —no slip/wall; left x —local stagnation pressure based on total head H_e over the spillway crest with a hydrostatic pressure distribution; and right x —continuative. The ogee-crest obstacle boundary was modeled as a smooth surface with no slip. With this configuration, the flow moves left to right, parallel with the slip walls, and between the no-slip floor and dam and the atmospheric pressure boundary at the top. Note that the free slip on the side walls was only for the 2D models. The 3D model's sidewalls were defined as no slip walls. Free slip is defined as a zero normal velocity component with zero tangential velocity derivatives. In the case of the free slip sidewalls, this gives $v = 0$ and $\partial u/\partial x = \partial w/\partial z = 0$. No slip is defined as zero tangential and normal velocities ($u = v = w = 0$). With a no-slip boundary, it is assumed that a law-of-the-wall type profile exists in the boundary region. A 1/7 power law is used to approximate the logarithmic law-of-the-wall expression. Wall shear stresses are thereby applied to the dam

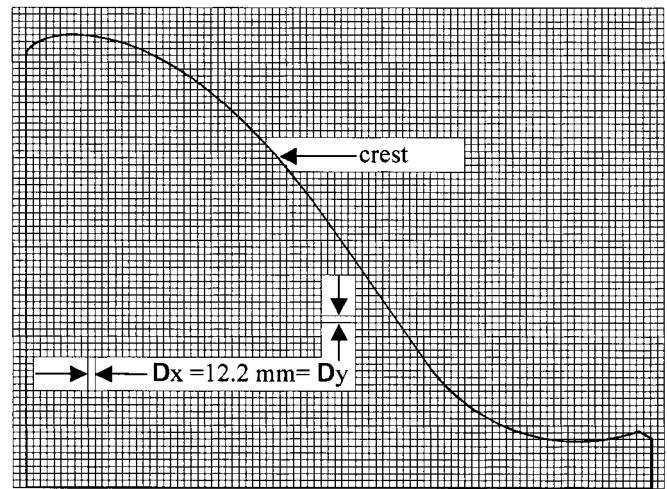


FIG. 2. Pressure Tap Locations on Physical Model, Numerical Model, and USACE Nomograph

surface using local Reynolds numbers and an algorithm taking into account the available fractional flow area (*Flow-3D* 1999).

The inflow boundary condition (left boundary, x -direction) can be computed with one of two pressure boundary conditions, static and stagnation. Both conditions employ a hydrostatic pressure distribution throughout the depth. The basic difference is that the stagnation condition assigns a zero velocity ($u = 0$) at the boundary and requires a pressure drop across the boundary for flow to occur. The static boundary condition defines the pressure as essentially continuous ($\partial P/\partial x = 0$) across the boundary, and the velocity at the boundary is assigned a value based on a zero normal-derivative condition across the boundary, $\partial u/\partial x = 0$ (*Flow-3D* 1999). In essence, for the hydrostatic stagnation condition, $P_{bc} = H_e$ with $u = 0$, and for the static condition, $P_{bc} = H_0$ with $u \neq 0$.

In some applications, the approach velocity may be non-significant and therefore omitted. This is done by replacing the total head H_e in (1) with the piezometric head H_0 . However, because the physical model was constructed in a flume, the approach velocity was significant at the higher flows. The presence of an approach velocity indicates that a static boundary condition should be used. However, because the static boundary condition uses the velocities adjacent to the boundary to calculate the boundary velocities, it can generate some numerically possible but physically unrealistic velocity profiles. For example, initializing a grid with velocities interpolated from a coarse grid could introduce slight errors that may continue to propagate in the solution. This result was found in several initial attempts; the flow had developed in two regimes. There was a low velocity region, upstream and below the crest of the dam, and a high velocity region, skimming over the low velocity and continuing over the dam.

To circumvent this instability, a stagnation boundary was used, which fixed the upstream boundary in time. But because the flow rate is unknown, it also required that an iterative method be employed. By defining the upstream boundary as the total head, the piezometric head measured in the physical model was increased by the velocity head H_v , giving the total head ($H_e = H_0 + u^2/2g$). The total head H_e was updated as the flow rate was refined. Visually, it can be seen in the numerical model that the extra velocity head depth H_v drove the flow and established a practical velocity profile within a few cells downstream. This iterative method fit very well with the manual multigrid method used for convergence.

An alternative method to the above method was found by first using a stagnation boundary condition for one or two grid refinements and then using a static boundary condition. At this

point, the velocity profile and grid refinement was sufficiently developed to prevent an unrealistic velocity profile from developing.

PHYSICAL MODEL

Description

A physical model of a typical ogee spillway, as shown in Fig. 1, with a design head H_d of 301 mm was fabricated and tested at the UWRL. The model was constructed of Plexiglas and was fabricated to conform to the distinctive shape of an ogee crest. The model also included a tangent section and a typical flip bucket. Plexiglas was chosen because it could be fabricated with smooth curves and easily instrumented with pressure taps. The model was 1.83 m wide and approximately 0.80 m high. The P/H_d ratio (height of crest/design head) was 2.7.

The spillway model was placed in a flume measuring approximately 1.83 m wide by 12 m long by 1.22 m deep. The ogee section was installed in the flume in an area with Plexiglas sides so that flow could be observed. The flume had a flat bottom and was equipped with baffles and wave suppressors to provide a uniform approach flow.

To ensure that sidewall effects did not influence the pressure data, the main pressure taps were located at the center of the sectional model (approximately 0.92 m from either sidewall). To assess whether or not there were sidewall effects, several pressure taps were placed laterally across the model crest axis and were observed during testing. Testing showed that the pressure taps located centrally on the model were not affected by the sidewalls of the flume. However, a tap that was located approximately 305 mm away from the sidewall of the flume was influenced by sidewall effects. Injection of dye showed corner vortices between the dam and the sidewall. The formation of the vortices initiated at the dam's face and continued over the crest. The vortices only affected the near-wall flow.

To ensure that the center taps would not interfere with adjacent downstream taps, the taps were staggered laterally. Every third tap was placed in the center of the spillway with the other two taps placed on either side. The tap spacing was approximately 150 mm apart in the flow directions and staggered approximately 150 mm. Fig. 3 shows the location of the pressure taps along the spillway.

Test Facilities

Water was supplied to the UWRL by means of gravity flow from First Dam, an impoundment located on the Logan River. Flow rates were measured using weight tanks, volumetric

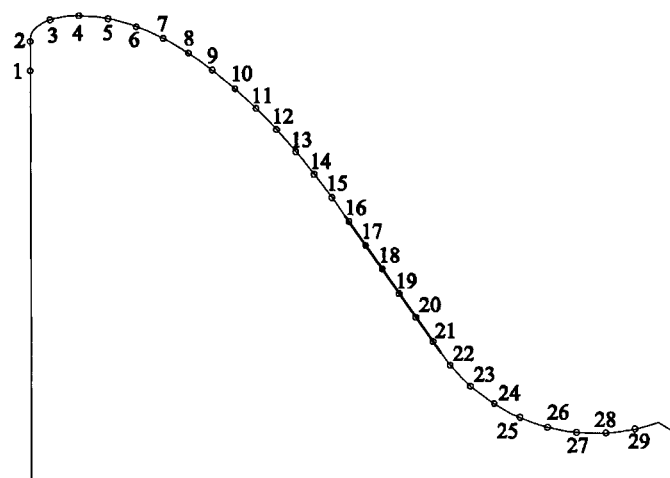


FIG. 3. Grid Dimensioning for Ogee Crest

tanks, or ultrasonic flowmeter. The method used was based on the flow quantity. For small flows, the weight tanks were used, whereas larger flows were measured with the volumetric tanks. The weight and volumetric tanks are NIST traceable with an accuracy of $\pm 0.25\%$. At the highest two flow rates, when the flow rate exceeded the capacity of the floor channel leading to the weight and volumetric tanks, a calibrated ultrasonic flowmeter was used. The accuracy of the flowmeter is $\pm 0.5\%$.

Pressures on the spillway were measured using a piezometer board with glass tubes vented to the atmosphere. The piezometer board was leveled and connected to the individual pressure taps. The piezometer board readings provided the average pressure reading at each pressure tap location. Measurements on the piezometer board were readable to within 1.3 mm. Because pressures fluctuated temporally along the crest, most likely due to surface waves, an average pressure was recorded.

Model Operation

A control valve was used to set the flow in the model. The model was operated at 10 different reservoir elevations ranging from $H_e/H_d = 0.07$ to 1.20, where H_e is the effective head upstream above the crest. To prevent the tailwater from interfering with the spillway pressure taps, free discharge from the flip bucket to the flume was allowed. For all test cases, the tailwater was kept below critical depth and had no influence on the pressure taps on the spillway. The headwater elevation was measured at a distance of 2.04 m upstream from the model crest.

RESULTS

The main purpose of this study was to compare results from a physical model with that of a numerical model for flow over an uncontrolled ogee crest. Existing USACE and USBR data have also been added as a comparison to existing references and as a convenience to the reader.

An evaluation of the pressure tap data from the physical model indicated that 3D effects are relatively small and only influence the flow near the wall. It was observed visually that there was a slight rise in the water surface elevation near the wall, due to the viscous effect of the wall. Using the numerical model, one flow rate was computationally modeled in three dimensions. Similar to the physical model, an increase in water surface elevation was noted near the wall. It was also noted that pressures changed laterally across the crest. However, the variation was not significant. A comparison of the discharge coefficients for this flow rate ($H_e/H_d = 0.87$) resulted in the discharge coefficient being 0.743 for the physical model, 0.740 for the 3D computational model, and 0.745 for the 2D computational model. Based on this comparison, it was determined that 2D analysis was sufficient and computationally faster.

The results have been nondimensionalized to allow a comparison in their simplest form. The design parameters— H_d = design head (m) and Q_d = design flow rate per unit length [$\text{m}^3/(\text{s} \cdot \text{m})$ —from the physical model are used as the basis. The design head was set at 0.301 m and the corresponding design flow, as determined from the model, was $0.376 \text{ m}^3/(\text{s} \cdot \text{m})$.

Fig. 4 shows the discharge relationships. The effective head H_e , which includes the velocity head, is nondimensionalized by the design head H_d and shown on the abscissa. The discharge Q is nondimensionalized by Q_d and shown on the ordinate. The actual nondimensional discharge values are included in the inset. Using the physical model and its discharge as the observed standard, the relative percent error in discharge is calculated and shown in Fig. 5. The relative percent error, at a given H_e/H_d , is defined as $(Q_c - Q_m)/Q_m \times 100$, where Q_m is the discharge in the physical model and Q_c is the discharge in the numerical model or as interpolated from the

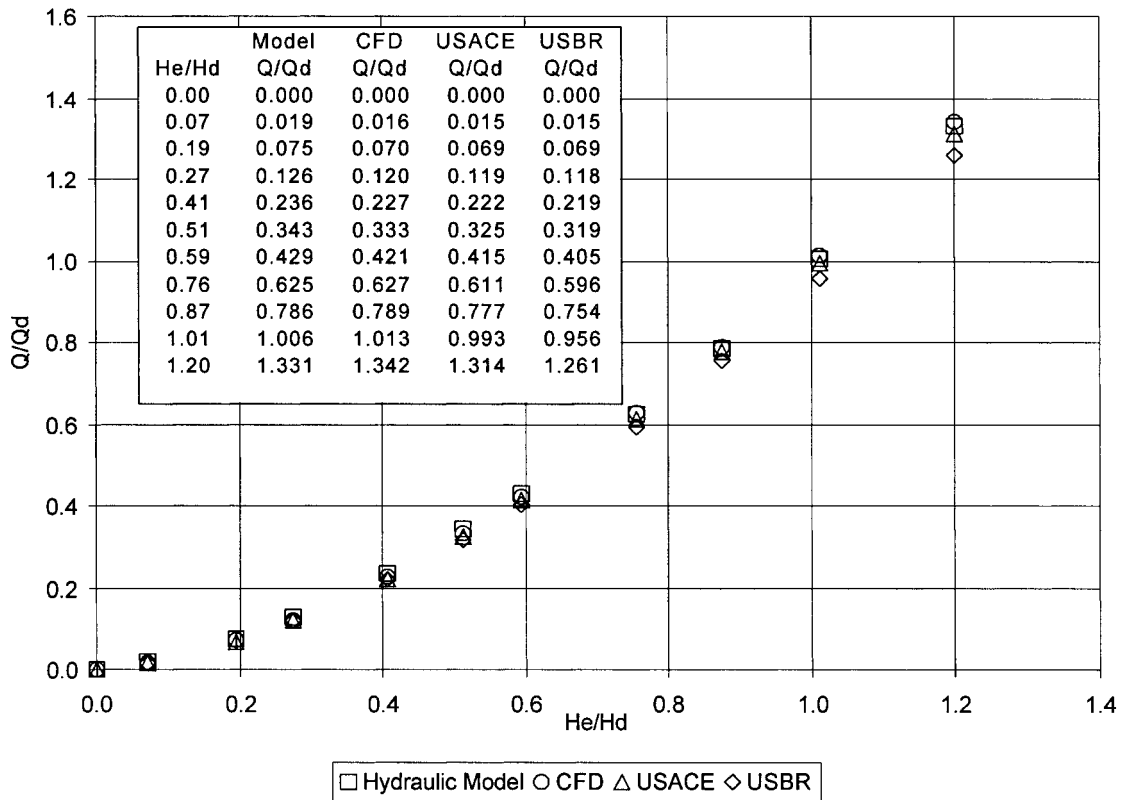


FIG. 4. Normalized Discharge Comparison

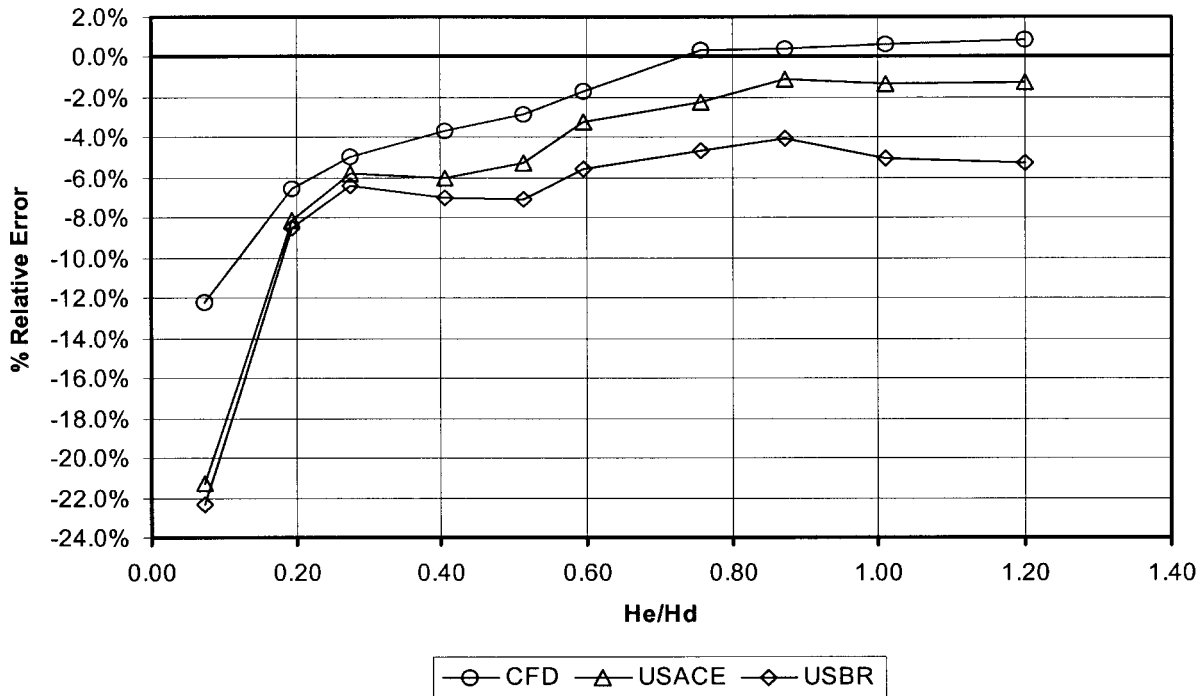


FIG. 5. Relative Percent Error in Discharge Using Physical Model as Basis

USBR or USACE design nomographs. The relative error shows that the numerical model agrees within 1% with the physical model for $H_e/H_d > 0.7$. The USACE discharge is similar to the numerical model but with a slight reduction accuracy. The USBR discharge shows the greatest deviation. The cause of the large deviation is most likely because the USBR crest is slightly different. The USBR upstream crest is shown as a compound curve consisting of two radii (*Design 1977*).

The physical model's upstream crest is constructed of three adjoining radii (Fig. 1). Other potential differing factors include primary flow measurement differences and crest construction. Many of the models test by the USBR and USACE were constructed using sheet metal. According to Maynard (1985), sheet metal may not bend in a true arc but in a series of small chords, which can lead to local variations of the pressures measured on the crest. However, the report also states

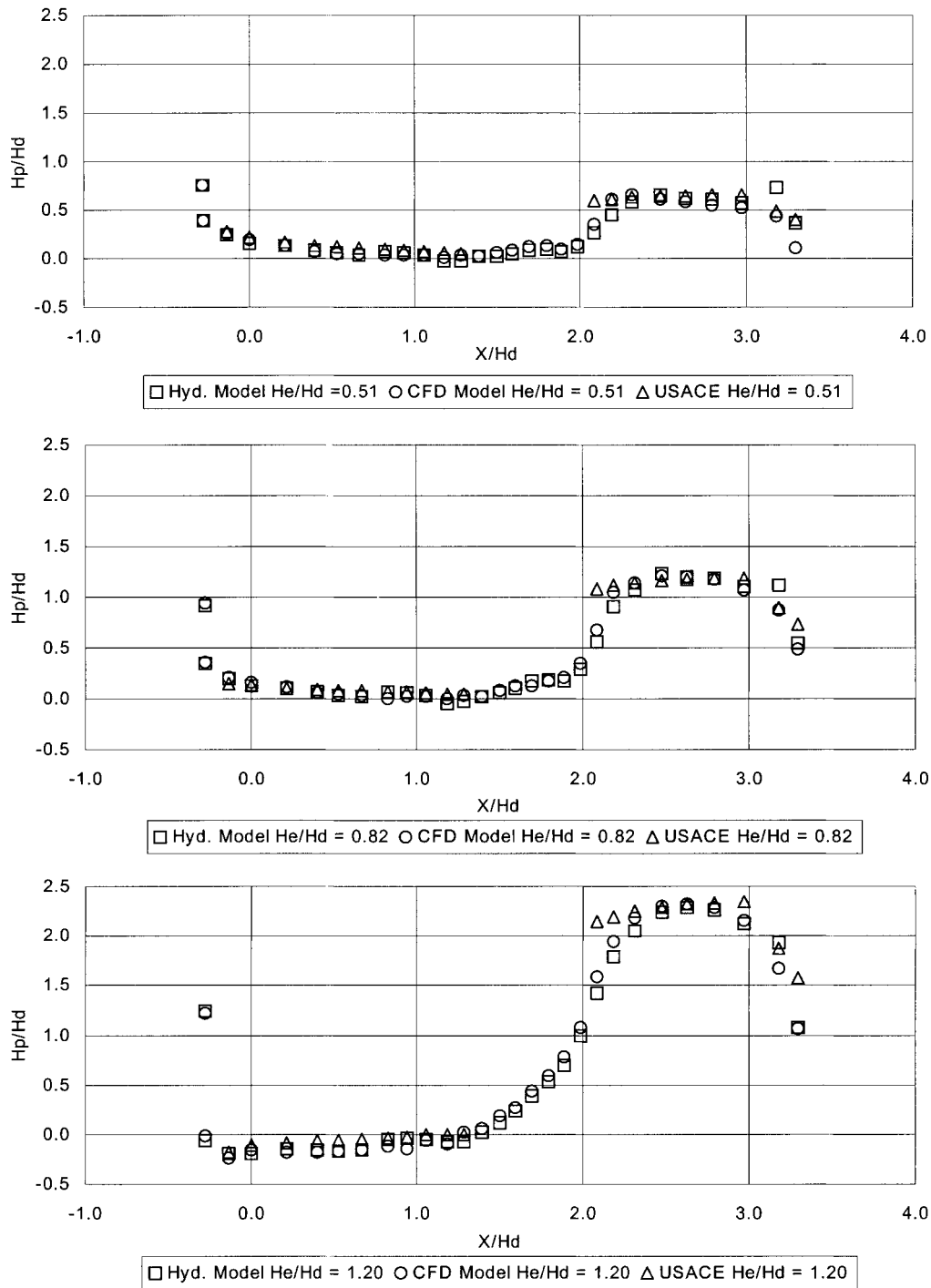


FIG. 6. Crest Pressure Comparison

that prototype construction methods may not provide any better relative tolerances.

Fig. 6 provides a comparison of average crest pressures for three different flow heads— $0.51H_d$, $0.82H_d$, and $1.20H_d$ —for the physical and numerical model. Crest pressures were interpolated at these heads from the USACE data (Maynard 1985). The pressure position on the spillway is shown nondimensionally as X/H_d , with X being the horizontal distance from the crest axis. The pressures are shown nondimensionally as H_p/H_d on the ordinate, where H_p is the pressure head. A comparison of the physical and the numerical model to either the USBR or the USACE data along the tangent was not possible because neither the USBR nor the USACE present this pressure data in their design nomographs. In fact, the

USACE indicates that model studies are likely required to obtain pressures on the tangent sections of spillways (USACE 1990).

Once again, using the physical model as the basis, Fig. 7 shows the absolute pressure error (cm) of water for the numerical model and the USACE data at a given X/H_d position. The absolute pressure difference is defined as $\Delta P = H_{pc} - H_p$, where H_p is the pressure head in the physical model and H_{pc} is the calculated pressure head from the numerical model or interpolated from the USACE design nomograph. For the pressures, an absolute error is used instead of a relative error because many of the crest pressures are nearly atmospheric ($H_p = 0$). At pressures near zero, even a small difference can result in a large relative error. For example, if a pressure difference

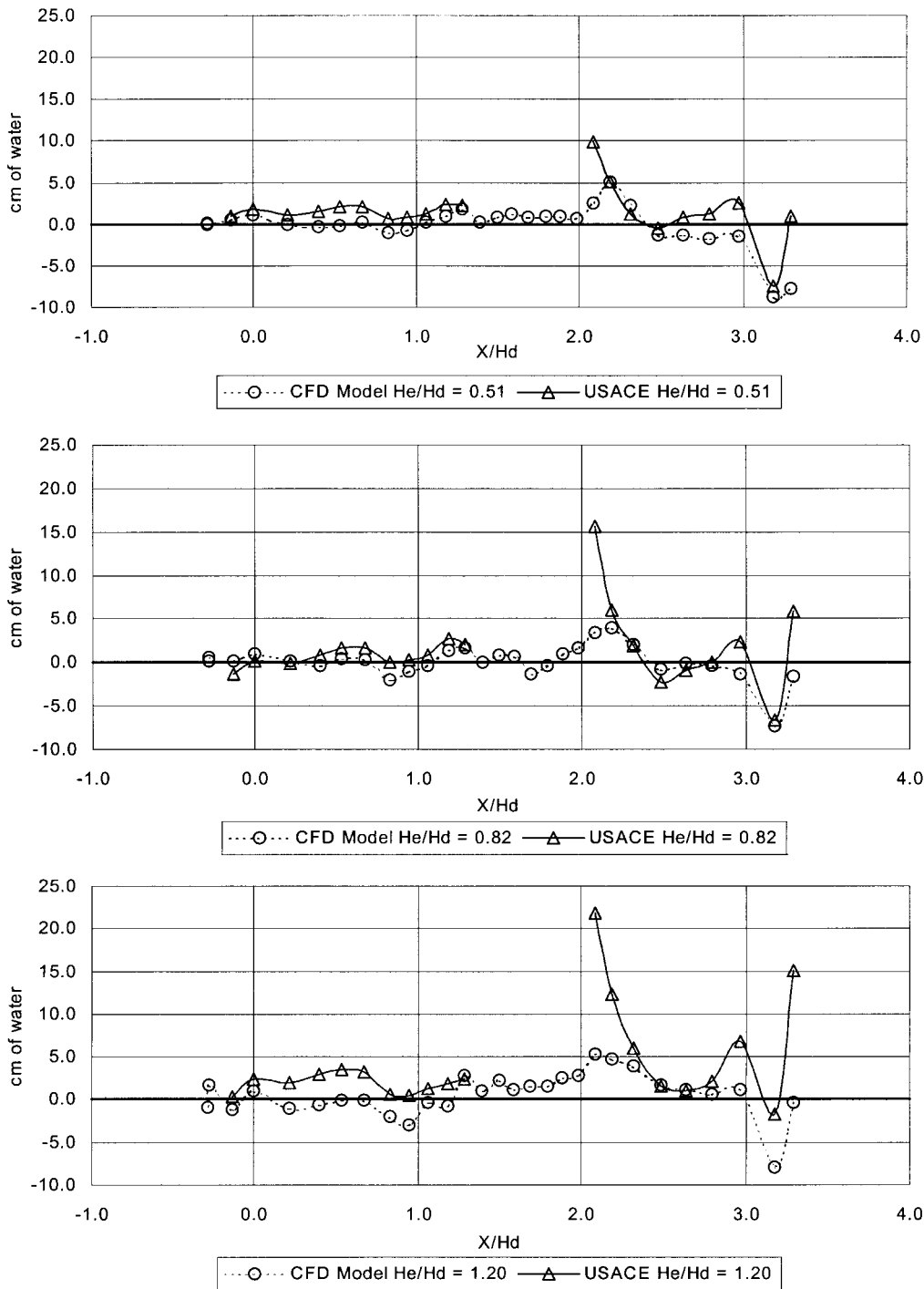


FIG. 7. Absolute Pressure Differences Using Physical Model as Baseline

of 1 cm of water was divided by a base pressure of 0.5 cm, a relative error of 200% would be calculated.

DISCUSSION

This study, in conjunction with the many previous studies, shows that, for uncontrolled flow over an ogee spillway, numerical tools are sufficiently advanced to calculate discharge and pressures on the spillway. New numerical techniques provide practicing engineers with an additional tool in the design or analysis of spillways. This tool may be very useful when reevaluating a dam for higher flows or improved hydrologic event flood calculations. It is apparent that, within the range tested, the numerical method has an improved accuracy over

the design nomographs for flow rates and pressures. However, the increased accuracy does not dictate that this method is sufficient or necessarily required for any given case. It is believed that the accuracy required is a question that must be answered on an individual basis.

Physical model studies are still considered the basis from which all other methods are compared. However, model studies may cost more and take more time to complete than a numerical study. If only approximate discharge and pressures are required, published design nomographs provide quick solutions that may be sufficient. As an alternative, numerical methods may offer accurate solutions, within given parameters, at a cost and time that may be less than model studies. Also, numerical models have the benefit of providing more

data, showing the entire discretized pressure and velocity fields.

In selecting a numerical method, it is important to understand the assumptions, simplifications, and parameters under which the numerical model is completed. For example, in this study, a temporal average (Reynolds averaging) was used to minimize the effects of rapid fluctuations. Although this appears to provide a good "average" solution, individual pressure spikes are not calculated. Note that, although the pressures reported from the physical model are also average crest pressures, fluctuating crest pressures are a real phenomenon. If pressure spikes are a concern, then a physical model should be considered.

Another concern in numerical modeling is the calculation of shock waves or the flow changing flow regimes. In general, it is easier to numerically model flow changing from subcritical to supercritical flow, rather than modeling flow changing from supercritical to subcritical, such as through a hydraulic jump. In this study, only the first scenario was used; therefore, no conclusion is drawn about the ability of this method to handle a hydraulic jump or shock waves on the downstream crest. For additional information on the difficulties in numerically modeling supercritical flow, the reader is referred to Rahman and Chaudry (1997), Krüger et al. (1998), and Causon et al. (1999).

With regard to the crest pressure data, caution should be exercised when a dam stability analysis is being completed. Although relatively close crest pressures were obtained from the physical and numerical model and the design nomographs, as shown in Figs. 6 and 7, a small change in a pressure applied over a large area can produce significantly different forces. Johnson et al. (1999) showed a 35% reduction in required posttensioned anchors for dam stability when comparing a model study with design nomograph data.

Although numerical tools still have limitations, there are many areas where current numerical methods may offer increased accuracy over design graphs and be sufficiently accurate for the required application. Numerical models can calculate pressure data on the tangent section, thereby allowing the hydrodynamic forces on an entire spillway to be calculated. In addition, these methods may allow the analysis of 3D ogee geometries, which are "sectional" only in cross section, to be completed. Often variables on some dams, such as P/H_d and the length of the tangent section, change from one end to the other. In the past, these types of dams have been analyzed as a set of parallel sectional dams. However, numerical methods offer the potential of analyzing the entire 3D flow field, which may provide a more accurate solution.

REFERENCES

- Betts, P. L. (1979). "A variation principle in terms of stream function for free surface flows and its application to finite element method." *Comp. and Fluids*, 7(2), 145–153.
- Bürgisser, M. F., and Rutschmann, P. (1999). "Numerical solution of viscous 2DV free surface flows: Flow over spillway crests." *Proc.*, 28th IAHR Congr., Technical University Graz, Graz, Austria.
- Cassidy, J. J. (1965). "Irrotational flow over spillways of finite height." *J. Engrg. Mech. Div.*, ASCE, 91(6), 155–173.
- Causon, D. M., Mingham, C. G., and Ingram, D. M. (1999). "Advances in calculation methods for supercritical flow in spillway channels." *J. Hydr. Engrg.*, ASCE, 125(10), 1039–1050.
- Chow, V. T. (1959). *Open-channel hydraulics*, McGraw-Hill, New York, 365–380.
- Colella, P., Graves, D. T., Modiano, D., Puckett, E. G., and Sussman, M. (1999). "An embedded boundary/volume of fluid method for free surface flows in irregular geometries." *Proc.*, 3rd ASME/JSME Joint Fluids Engrg. Conf., ASME Paper FEDSM99-7108, 9–14.
- Design of small dams*. (1977). U.S. Bureau of Reclamation, U.S. Government Printing Office, Washington, D.C.
- Flow-3D user manual; excellence in flow modeling software*, v 7.5. (1999). Flow Science, Inc., Santa Fe, N.M.
- Guo, Y., Wen, X., Wu, C., and Fang, D. (1998). "Numerical modeling of spillway flow with free drop and initially unknown discharge." *J. Hydr. Res.*, Delft, The Netherlands, 36(5), 785–801.
- Harlow, F. H., and Welsh, J. E. (1965). "Numerical calculation of time-dependent viscous incompressible flow of fluid with free surface." *Physics of Fluids*, 8, 2182–2189.
- Hirt, C. W. (1992). "Volume-fraction techniques: Powerful tools for flow modeling." *Flow Sci. Rep. FSI-92-00-02*, Flow Science, Inc., Santa Fe, N.M.
- Hirt, C. W., and Nichols, B. D. (1981). "Volume of fluid (VOF) method for the dynamics of free boundaries." *J. of Computational Physics*, 39, 201–225.
- Hirt, C. W., and Sicilian, J. M. (1985). "A porosity technique for the definition of obstacles in rectangular cell meshes." *Proc.*, 4th Int. Conf. Ship Hydro., National Academy of Science, Washington, D.C., 1–19.
- Ikegawa, M., and Washizu, K. (1973). "Finite element method applied to analysis of flow over a spillway crest." *Int. J. Numer. Methods in Engrg.*, 6, 179–189.
- Johnson, M. C., King, J. R., and Scanlon, J. W. (1999). "Inks dam modernization project." *Dealing with Aging Dams, 19th Annual USCOLD Lecture Series*, U.S. Committee on Large Dams, Denver, 391–403.
- Kothe, D. B., and Mjolsness, R. C. (1992). "RIPPLE: A new model for incompressible flows with free surfaces." *AIAA J.*, 30(11), 2694–2700.
- Krüger, S., Bürgisser, M., and Rutschmann, P. (1998). "Advances in calculating supercritical flow in spillway contractions." *Proc.*, *Hydroinformatics 1998*, Vol. 1, V. Babovic and L. Larsen, eds., Balkema, Rotterdam, The Netherlands, 163–170.
- Li, W., Xie, Q., and Chen, C. J. (1989). "Finite analytic solution of flow over spillways." *J. Engrg. Mech.*, ASCE, 115(12), 2635–2648.
- Maynard, S. T. (1985). "General spillway investigation." *Tech. Rep. HL-85-1*, U.S. Army Engineer Waterways Experiment Station, Vicksburg, Miss.
- Murphy, T. E. (1973). "Spillway crest design." *MP H-73-5*, U.S. Army Engineer Waterways Experiment Station, Vicksburg, Miss.
- Nichols, B. D., and Hirt, C. W. (1975). "Methods for calculating multi-dimensional, transient free surface flows past bodies." *Proc.*, 1st Int. Conf. Ship Hydrodynamics, J. W. Schot and N. Salvesen, eds., Naval Ship Research and Development Center, Bethesda, Md., 253–277.
- Nichols, B. D., Hirt, C. W., and Hotchkiss, R. S. (1980). "Volume of fluid (VOF) method for the dynamics of free boundaries." *Los Alamos Scientific Lab. Rep. LA-8355*, Los Alamos, N.M.
- Olsen, N. R., and Kjellesvig, H. M. (1998). "Three-dimensional numerical flow modeling for estimation of spillway capacity." *J. Hydr. Res.*, Delft, The Netherlands, 36(5), 775–784.
- Rahman, M., and Chaudry, H. M. (1997). "Computation of flow in open-channel flow." *J. Hydr. Res.*, 35(2), 243–256.
- Rodi, W. (1980). "Turbulence models and their application in hydraulics." *Monograph*, International Association for Hydraulic Research, Delft, The Netherlands, 27–30.
- U.S. Army Corp of Engineers (USACE). (1990). "Hydraulic design of spillways." *EM 1110-2-1603*, Dept. of the Army, Washington, D.C.
- Versteeg, H. K., and Malalasekera, W. (1995). *An introduction to computational fluid dynamics*, Longman Scientific and Technical, New York.
- Yakhot, V., and Orszag, S. A. (1986). "Renormalization group analysis of turbulence. I. Basic theory." *J. Scientific Computing*, 1(1), 1–51.
- Yakhot, V., and Smith, L. M. (1992). "The renormalization group, the ϵ -expansion and derivation of turbulence models." *J. Scientific Computing*, 7(1), 35–61.
- Yamada, F., and Takikawa, K. (1999). "Improving the accuracy of free-surface recognition and conservation of mass for the volume of fluid method." *Proc.*, *Int. Offshore and Polar Engrg. Conf.*, Vol. 3, International Society of Offshore and Polar Engineering (ISOPE), Cupertino, Calif., 643–650.

NOTATION

The following symbols are used in this paper:

- A_j = area of cell face in j -direction;
 C_0 = nondimensional discharge coefficient;
 f_i = Reynolds stresses;
 g_i = acceleration due to gravity in i -direction;
 H_d = design head;
 H_e = total head above crest;
 H_o = static head above crest;
 H_p = pressure head;

H_{pc} = calculated or interpolated pressure head;
 H_v = velocity head, $u^2/2g$;
 L = lateral length of crest;
 P = height of dam at crest axis;
 P' = mean hydrodynamic pressure;
 P_{bc} = pressure at boundary condition;
 Q = discharge rate;
 Q_d = discharge rate at design head;

U_j, U_i = velocity in i - and j -directions;
 u = velocity in x -direction;
 V_F = volume of fluid in cell;
 v = velocity in y -direction;
 w = velocity in z -direction;
 X = horizontal distance from crest axis;
 x_i, x_j, x, y, z = spatial coordinates; and
 ρ = fluid density.